Anharmonic decay time, isotopic scattering time, and inhomogeneous line broadening of optical phonons in ^{70}Ge, ^{76}Ge, and natural Ge crystals

H. D. Fuchs, C. H. Grein, R. I. Devlen, J. Kuhl, and M. Cardona
Max-Planck-Institut für Festkörperforschung, Heisenbergstrasse 1, D-7000 Stuttgart 80, Federal Republic of Germany
(Received 30 May 1991)

High-accuracy (0.02-cm^{-1}) first-order Raman spectra of two different isotopically enriched Ge crystals (95.9% ^{70}Ge and 86.0% ^{76}Ge) and a Ge crystal of natural isotopic composition as well as time-resolved picosecond Raman spectra of the isotopically enriched ^{70}Ge and natural Ge were measured and compared with theoretical calculations using the self-consistent Born approximation and the coherent-potential approximation. The broadening of the Raman line in the frequency domain was found to be predominantly caused by the anharmonic decay of optical phonons into lower-energy acoustic phonons, resulting in a line broadening that is inversely proportional to the average isotopic mass $\overline{m}$. Isotopic disorder contributes only a little to the line broadening and depends on the isotopic composition of the material. From the phonon linewidths the anharmonic decay time of optical phonons in Ge at 80 K was determined to be $\overline{m}(8.4\pm0.1)\times10^{-2}$ ps ($\overline{m}$ is the average isotopic mass in atomic-mass units). The isotopic (elastic) scattering time of optical phonons depends strongly on the isotopic composition and is two orders of magnitude longer than the decay time in all samples. The asymmetry observed in the Raman lines is explained in terms of the opacity of the material and the asymmetric phonon self-energies (due to isotopic disorder). The decay time of the time-resolved incoherent anti-Stokes Raman signal is 8 ± 1 ps for both the isotopically enriched and the natural Ge. It is suggested that the discrepancy between the *phonon* decay time (determined from the frequency-domain measurements) and the nonequilibrium *phonon population* decay time (determined from the time-domain measurements) is due to effects related to the phonon-generation process in the transient experiment.

I. INTRODUCTION

The dynamics of phonons in semiconductor crystals has attracted considerable interest in the past from both theoretical and experimental points of view.[1–14] Two processes induce lifetime broadening of optical phonons in crystalline materials: (i) spontaneous anharmonic (inelastic) decay in which a phonon is converted into lower-energy phonons (decay time τ_{decay}, which is sometimes also referred to as T_1) and (ii) elastic scattering arising from the distribution of isotopic masses and defects. Because of the low concentration of free carriers in our samples ($\leq4\times10^{16}$ cm^{-3}) and the high quality of the crystals, only the inhomogeneous broadening due to isotopic scattering was taken into account in this work (isotopic scattering time τ_{isotope}, sometimes also referred to as T_2).

Isotopic disorder does not only influence the lifetime of phonons, measured by the inverse of the phonon linewidth in vibrational spectra, but also causes an asymmetry of the line shape and a shift of the phonon energy in Raman spectra.

For high-energy *acoustic* phonons, Tamura calculated the anharmonic decay rates (in the isotopic model in terms of the second- and third-order elastic constants) and the elastic isotopic scattering times in Ge (using a Born–von Kármán model of lattice dynamics and the first Born approximation).[1,2] A scaling theory was developed by Kazakovtsek and Levinson and others[3–5] to describe nonequilibrium acoustic-phonon propagation in a crystal under the implicit assumption that the anharmonic decay time is larger than the isotopic scattering time (the theory is based upon the diffusion equation). Maris,[6] however, has recently shown that this theory may be invalid in the usual case in which the elastic scattering arises only from the various naturally occurring isotopes. His Monte Carlo calculations suggest a fairly large probability that hot acoustic phonons injected in a Ge crystal decay into lower-energy phonons, which then reach the detector (at a distance of say 1 cm) ballistically, i.e., without any further scattering.

For *optical* phonons the first calculations of phonon lifetimes go back to 1965 when Cowley computed the optical-phonon decay time in Ge, summing over all possible decay processes.[7] He described the anharmonic interaction in terms of an axially symmetric force between nearest neighbors and obtained the parameters for this interaction by fitting the calculated thermal-expansion coefficients to experimental data.[7] A simplified treatment of the phonon decay times, only considering the decay of optical phonons into two acoustic phonons with opposite wave vector which belong to the same branch, was given by Klemens.[8]

After short-pulse lasers became available, it was possible to obtain information about the phonon dynamics directly from time-resolved experiments. Using time-resolved incoherent picosecond anti-Stokes Raman spectroscopy,[9] the temporal evolution of nonequilibrium optical-phonon populations can be determined. The nonequilibrium phonon population is generated by cooling of photoexcited carriers and decays by inelastic

scattering of the phonons.

In natural Ge, Ye, Roxlo, and Genack[10] found phonon-population decay times of 8±1 ps at 105 K and 5±1 ps at 300 K and pointed out that these decay times were consistently longer than the corresponding inverse Raman linewidths. The difference between time- and frequency-domain measurements has been attributed to elastic (isotopic) scattering of the optical phonons.[10] Young, Wan, and van Driel,[11] on the other hand, reported phonon-population decay times of 8±1 ps at 77 K and 4±1 ps at 300 K, but concluded that there is no significant discrepancy between the phonon lifetimes as determined in the time and frequency domains, given the range of values for phonon linewidths that can be found in the literature.[11] Recently, Fuchs *et al.* compared measurements of the phonon spectra of isotopically pure ^{70}Ge with those of natural Ge taken under identical conditions.[12] There was no observable difference in the linewidths between the isotopically pure and the natural materials. These results were in general agreement with measurements by Agekyan *et al.* who compared spectra of ^{76}Ge with natural Ge.[13] Because there has been no observable line broadening due to isotopic disorder, the linewidth of optical-phonon spectra, meaning the lifetime of optical phonons in a crystal, was expected to be predominantly determined by anharmonic decay.

In the present work, we were able to determine the anharmonic decay time τ_{decay} of optical phonons and the isotopic scattering time τ_{isotope} with high accuracy. In a direct and unambiguous way, τ_{decay} was shown to be two orders of magnitude smaller than τ_{isotope}. It was possible to reach this conclusion by comparing the linewidths of phonon spectra from two different isotopically enriched samples (85.9% ^{70}Ge and 86.0% ^{76}Ge) with those of natural Ge and separating the mass-dependent part of the linewidths (anharmonic decay[15]) from the mass-independent part (isotopic scattering).

Additionally performed picosecond Raman measurements have yielded the same decay time of photoexcited nonequilibrium phonon populations for natural Ge and isotopically enriched ^{70}Ge. This means that, within the experimental uncertainty of the measurement, the decay time of the phonon population is independent of the isotopic composition in the material. However, the *phonon-population* decay times measured in the picosecond experiments were consistently longer than the *phonon* decay times determined from Raman linewidths. Since anharmonic decay produces the largest contribution to the Raman linewidth, elastic scattering (to which the picosecond experiment is not sensitive) cannot be the origin of this difference. To account for the discrepancy between the time- and frequency-domain measurements, the dynamics of phonon generation in the picosecond experiment are considered. This means that, in contrast to the work of Ye, Roxlo, and Genack[10] and Young, Wan, and van Driel,[11] the decay time of the nonequilibrium *phonon population* is not simply the *phonon* decay time, but a phonon-generation time is taken into account to explain the fact that the nonequilibrium phonon population decays more slowly than the phonons; this follows from a comparison of frequency- and time-domain measurements.

We also analyzed the line shape of the first-order Raman spectra of the different Ge samples and found an asymmetric broadening, depending on the isotopic composition of the materials. Contributions to the asymmetry arising from isotopic disorder and absorption of the laser light in the material are discussed. For Brillouin scattering, it is well known that the opacity of a material results in asymmetric phonon lines, and different models have been suggested to describe this behavior.[16–19] *Optical* phonons are much less dispersive than *acoustic* ones, and so far disorder-induced asymmetric Raman line shapes of semiconductors have only been observed in alloys. This work, however, shows that even in isotopically enriched materials both the opacity of the material as well as the isotopic disorder contribute to the asymmetry of the first-order Raman line shape. The experimentally observed asymmetry of the phonon lines, as well as their relative energy shifts, are compared to calculations based on the self-consistent Born approximation (SCBA) and the coherent-potential approximation (CPA).

II. THEORY

A. Isotopic disorder effects

Isotopic disorder influences the phonon energies as well as the width and shape of Raman lines. Scattering is treated in the coherent-potential approximation by considering the disordered material as an "effective" medium, characterized by the dimensionless "self-energy" $\tilde{\epsilon}(\omega)$ (ω is the phonon frequency) with respect to the virtual crystal (VC). In our case the VC was defined to be a perfect diamond-structure crystal with each site occupied by a Ge atom of average atomic mass $\bar{m}$. The CPA predicts a negligibly small *line broadening* due to isotopic disorder for first-order Raman lines, because the phonon density of states approaches zero at the Γ point.[12] Calculations using the self-consistent Born approximation have also been performed. The zone-center optical-phonon self-energy in the SCBA is given by

$$\Pi=\Pi_r+i\Pi_i\ , \tag{1}$$

where

$$\Pi_r(\omega_{\Gamma\text{op}})\approx\frac{\omega_{\Gamma\text{op}}^2 g_2}{24N}\sum_{\mathbf{q}j}\frac{2\omega_{\mathbf{q}j}}{\omega_{\Gamma\text{op}}^2-\omega_{\mathbf{q}j}^2-2\omega_{\mathbf{q}j}\Pi_r(\omega_{\Gamma\text{op}})}\ , \tag{2}$$

$$\Pi_i[\omega_{\Gamma\text{op}}+\Pi_r(\omega_{\Gamma\text{op}})]\approx-\frac{\pi\omega_{\Gamma\text{op}}^2 g_2}{24}\text{Re}\rho\{\omega_{\Gamma\text{op}}-i\Pi_i[\omega_{\Gamma\text{op}}+\Pi_r(\omega_{\Gamma\text{op}})]-i\Gamma_p\}\ , \tag{3}$$

where $\omega_{\mathbf{q}j}$ is the frequency of a branch j phonon with wave vector $\mathbf{q}$ ($\omega_{\Gamma\text{op}}$ is the optical phonon at the zone center), g_2 is defined in Eq. (10), ρ is the phonon density of states, N is the number of unit cells in the sample, and Γ_p the broadening due to anharmonic decay. These equations yield an isotopic-disorder contribution to the

full width at half maximum (FWHM) of only 0.017 cm^{-1} for Ge of natural isotopic composition.[12] Expressed in terms of phonon lifetimes (inversely proportional to the linewidths), these calculations suggest that the isotopic scattering time of optical phonons in Ge crystals is considerably longer than the total phonon lifetime.

The *energy shift* of the zone-center optical phonons in natural Ge with respect to its VC energy, caused by isotopic disorder, has been calculated with the CPA to be 1.5 cm^{-1} (Ref. 12) and is 0.98 cm^{-1} in the SCBA [Eq. (2)].

Using the phonon self-energy $\tilde{\epsilon}(\omega)$ obtained from the CPA, the contribution of isotopic disorder to the *asymmetry* of first-order Raman lines can be calculated. Within the framework of CPA, the Raman line shape can be written as

$$I(\omega^2)=-\mathrm{Im}\{\omega^2[1-\tilde{\epsilon}(\omega)]-\omega_{\mathrm{Top}}^2+2i\omega\Gamma_p/\hbar\}^{-1} . \quad (4)$$

The Raman intensity of natural Ge shown in Fig. 1 was calculated with Eq. (4) using the phonon self-energies of Ref. 12. The dashed line in Fig. 1 indicates the symmetric part of the spectrum. The asymmetry of the Raman line, resulting from the self-energy contributions due to isotopic disorder, depends on the isotopic composition of the material and is therefore expected to be different for each of the three Ge samples.

Thus all three isotopic disorder effects, the broadening, renormalization of the phonon energies, and asymmetry of the Raman lines, can be explained with the CPA and SCBA. These results will be compared with experiment in Sec. IV.

B. Opacity of the material

Several models have been suggested to describe asymmetric *Brillouin* lines arising from the opacity of the material,[16–19] but in *Raman* scattering the opacity of the material has previously not been taken into account as having an influence on the line shape. To analyze the data presented in this work, a phenomenological one-dimensional model was used.[20] Modes not only from the zone center, but with a Lorentzian q distribution of half-width ξ, were assumed to contribute to the Raman line

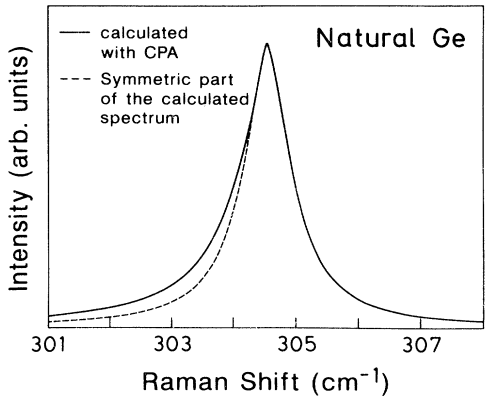

FIG. 1. Calculated first-order Raman intensity of natural Ge. The isotopic disorder was taken into account using the coherent-potential approximation (CPA) [Eq. (1)].

(the relation between ξ and the absorption coefficient α is discussed in Sec. IV A). Every one of these modes has a Lorentzian line shape of half-width γ around the frequency $\omega(q)$. The Raman intensity $R(\omega)$ is thus the weighted sum of these lines:

$$R(\omega)\propto\int_0^{2\pi/a}P(q)\frac{2\gamma/\pi}{[\omega-\omega(q)]^2+\gamma^2}dq . \quad (5)$$

Here a is the lattice constant of Ge and the optical-phonon dispersion $\omega(q)$ is approximated by

$$\omega(q)=\omega_0-Bq^2 , \quad (6)$$

where the parameter B is obtained from neutron-scattering data.[21] The wave-vector distribution $P(q)$ is written as

$$P(q)=\frac{2\xi/\pi}{q^2+\xi^2} . \quad (7)$$

Carrying out the integral of Eq. (5) in the complex plane leads to the Raman intensity of the form

$$R_{\xi\gamma}(\omega)=\frac{\gamma[(\omega-\omega_0)^2+\gamma^2]^{1/2}-\sqrt{B}\,\xi(\omega-\omega_0-B\xi^2)(\{[(\omega-\omega_0)^2+\gamma^2)]^{1/2}-(\omega-\omega_0)\}/2)^{1/2}}{[(\omega-\omega_0)^2+\gamma^2]^{1/2}\{[(\omega-\omega_0)-B\xi^2]^2+\gamma^2\}}$$

$$-\frac{\gamma\sqrt{B}\,\xi(\{[(\omega-\omega_0)^2+\gamma^2]^{1/2}+(\omega-\omega_0)]\}/2)^{1/2}}{[(\omega-\omega_0)^2+\gamma^2]^{1/2}\{[(\omega-\omega_0)-B\xi^2]^2+\gamma^2\}} . \quad (8)$$

Equation (8) describes the asymmetric line shape obtained from modes with half-width γ whose wave-vector distribution is a Lorentzian with half-bandwidth ξ. Least-squares fits of Eq. (8) to the experimental results (shown in Fig. 3) will be discussed in Sec. IV.

III. EXPERIMENT

A. Experimental details

The germanium sample of natural isotopic composition was cut in the (111) orientation from a high-purity n-type

TABLE I. Isotopic composition of isotopically enriched ^{70}Ge, ^{76}Ge, and natural Ge used in this experiment.

Isotope	Mass[a] (atomic units)	Atomic percent Isotop. enriched ^{70}Ge	Isotop. enriched ^{76}Ge	Natural Ge
70	69.9243	95.9		20.5
72	71.9217	3.8	0.1	27.4
73	72.9234		0.23	7.8
74	73.9219		13.7	36.5
76	75.9214		86.0	7.1

[a]Reference 30.

single crystal. The purification of the material and growth of the isotopically enriched n-type ^{70}Ge crystal was described in Ref. 12. The material for the p-type ^{76}Ge sample was isotopically enriched by Eagle Picher (Quapaw, OK), and the crystal was then grown by Ortec (Livermore, CA). The carrier concentration of the crystals as determined from Hall measurements was found to be $N_d - N_a \approx 2\times10^{13}$ cm^{-3} for the natural Ge, $N_d - N_a \approx 4\times10^{16}$ cm^{-3} for ^{70}Ge, and $N_a - N_d \approx 4\times10^{11}$ cm^{-3} for ^{76}Ge at 80 K, insufficient to affect the phonon spectra.[22] The values for the isotopic composition of the Ge samples used in this experiment, as obtained by means of mass spectroscopy, are given in Table I.

The chemomechanically polished surface of all Ge samples was cleaned with diethyl-ether and acetone prior to measurements being taken. Unpolarized Raman spectra were recorded in a backscattering geometry at liquid-nitrogen temperature using the discrete 514.5-nm line of an Ar^+ laser with an étalon placed in the cavity.

The high accuracy of the results reported in this work was achieved by measuring in the tenth diffraction order of the grating (316 lines/mm) of a 2.12-m SOPRA double monochromator (single-pass configuration) and detecting the dispersed light with photon-counting techniques (photomultiplier). An estimate for the uncertainty of the results was obtained by measuring the FWHM of the laser line with the same slit apertures as the Raman experiment. The so-obtained FWHM for the laser line indicated an uncertainty of about 0.02 cm^{-1} for this experiment.

To measure directly the temporal evolution of a nonequilibrium phonon population, we used time-resolved spontaneous anti-Stokes Raman scattering.[9] Laser pulses were generated in a synchronously mode-locked Rhodamine 6G dye laser operating at $\lambda = 592$ nm ($\hbar\omega = 2.1$ eV) with a repetition rate of 76 MHz and an average power of 100 mW. The pulse width was approximately 5 ps.

The output of the laser was split to form two beams of approximately equal intensity which were linearly and orthogonally polarized. The two beams which have a continuously variable time delay were focused to the same spot on the sample and the backward-scattered light detected by a standard photon-counting Raman spectrometer. The first beam (pump) generates electron-hole pairs (estimated density of a few times 10^{18} cm^{-3}) with a large excess energy ($\hbar\omega - E_{\rm gap} = 1.4$ eV at 80 K) whose initial return to equilibrium with the lattice is dominated by optical-phonon emission. The presence of a nonequilibrium phonon population is detected by the second, time-delayed, beam (probe) as an increase in its anti-Stokes signal. Only optical phonons generated in a small region of the Brillouin zone ($q \sim 0$) will be Raman detectable due to conservation of energy and momentum for the phonon-photon scattering event. Othonos *et al.*[14] have calculated that the appropriate phonons are generated predominantly by the relaxation of hot heavy holes.

We stress that the phonon-population decay time determined by this technique is that of the incoherent population. In particular, elastic-scattering events will result in a decreased lifetime when determined from frequency linewidth measurements, whereas these elastic-scattering events will not affect the phonon-population decay time, measured in the picosecond experiment.

B. Experimental results

The spectra of the first-order optical phonons for the isotopically enriched samples ^{70}Ge and ^{76}Ge as well as the natural Ge sample are shown in Fig. 2. These spectra are the average of three independent measurements for

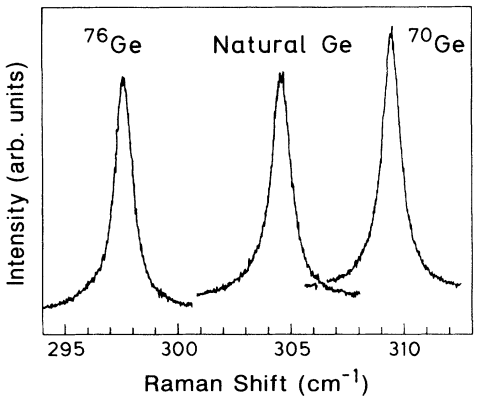

FIG. 2. Experimental first-order Raman spectra of isotopically enriched ^{76}Ge, ^{70}Ge, and natural Ge. The data were taken at 80 K in the tenth diffraction order of the grating with an excitation energy of $E_L = 2.41$ eV (Ar^+ laser with étalon).

TABLE II. Parameters of the experimental Raman spectra of isotopically enriched ^{70}Ge, ^{76}Ge, and natural Ge [obtained by fitting the data to Eq. (8)].

	FWHM of modes deconvoluted (cm^{-1})	Asymmetry parameter ξ (10^3 cm^{-1})	Phonon energy shift compared to natural Ge (cm^{-1})
^{76}Ge	0.84(±0.02)	725(±40)	7.01(±0.02)
Natural Ge	0.89(±0.02)	970(±50)	
^{70}Ge	0.90(±0.02)	610(±30)	4.91(±0.02)

each sample. The phonon lines for the samples of the different isotopic composition are well separated with the phonon energy in natural Ge being 4.91 cm^{-1} lower than in ^{70}Ge and 7.01 cm^{-1} higher than in ^{76}Ge (see Table II).

In addition to the frequency, also the width and asymmetry of the first-order Raman lines have been analyzed. The experimental spectra were fitted to a model which takes into account a Lorentzian distribution of the phonon wave vectors as described in Sec. II [Eq. (8)]. The asymmetry parameter ξ is the half-width of this wave-vector distribution, and the results for the three samples, as obtained from the fits, are listed in Table II.

It is noteworthy that even the isotopically enriched samples show an asymmetric shape of the first-order optical Raman lines. This can be clearly seen in Fig. 3, where the spectra of the different samples have been shifted in energy so as to place the peaks at the same position for the sake of comparison. The dotted lines are the least-squares fits of Eq. (8) to our data, and the dashed lines indicate the symmetric parts of the spectra. As will be discussed further in Sec. IV, the asymmetry of the lines arose from (i) the finite penetration depth of the laser light in the samples and (ii) the phonon self-energy asymmetry due to isotopic disorder.

The fits also gave the FWHM of the modes Δ_{mode}, which equals 2γ, where γ is a fit parameter in Eq. (8). Note that the spectra of Fig. 3 are the total Raman intensities which are, according to Eq. (8), the weighted sum of phonons whose wave vectors are slightly spread around the zone center. The linewidth of each mode (Δ_{mode}) contributing to the total Raman intensity is the quantity which was used to determine the phonon decay times. Even though the spectrometer allowed very accurate measurements, the finite resolution of the system had to be taken into account. Following the description given in Ref. 12, the fitted linewidths were deconvoluted with the instrumental broadening and the resulting deconvoluted linewidths (Δ_{mode}) are listed in Table II. The differences between the linewidths of the various Ge samples were quite small but because of the very high resolution of the system, we were able to measure an increasing Δ_{mode} with decreasing isotopic mass. As explained in Sec. IV, the difference of the Δ_{mode} was predominantly caused by the mass-dependent anharmonic decay of the optical phonons.

Figure 4 shows the time-resolved transients of the anti-Stokes Raman signals for natural Ge and ^{70}Ge at 80 K. Both samples have a (111) surface which yields a Raman signal for both polarizations of scattered light. Consequently, we could not discriminate against the anti-Stokes signal of one of the optical beams with a polarization analyzer. The resulting time-dependent signal is symmetric about zero time delay.

The amplitude of the time-dependent signal was 125 and 200 counts/s for the natural Ge and ^{70}Ge samples. We also observed a time-dependent signal away from the anti-Stokes line with a peak amplitude of 25 counts/s, which decayed to zero within 10 ps. We attribute this to hot luminescence.[23]

The data in Fig. 4 have been normalized and a constant background subtracted for ease of comparison. Although the ^{70}Ge transient exhibits a small decay before the signal

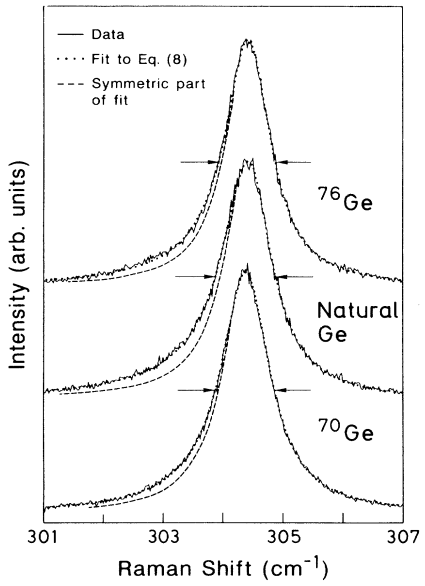

FIG. 3. Experimental first-order Raman spectra of isotopically enriched ^{76}Ge, ^{70}Ge, and natural Ge, taken at 80 K with an excitation energy of $E_L = 2.41$ eV. The spectra of ^{76}Ge and ^{70}Ge have been shifted in energy for the sake of comparison. The solid lines are experimental and dotted lines are fits to the asymmetric line shape described in the text [Eq. (8)]. The width, shape, and energy of the spectra are discussed in the text. (Note that these are the raw data, meaning the weighted sum of phonons whose wave vectors are slightly spread around the Brillouin-zone center [Eq. (8)]. The indicated widths are therefore not identical with the $\Delta_{\text{mode}} = 2\gamma$ of the individual modes in Fig. 6.)

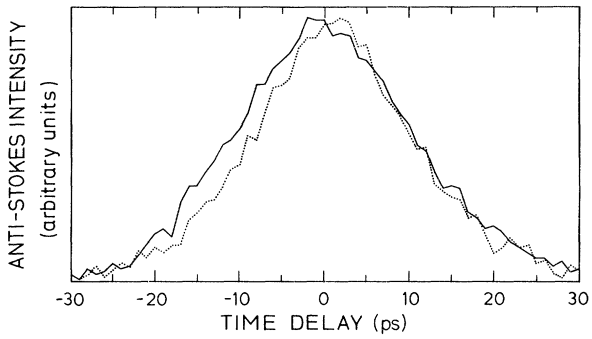

FIG. 4. Time-resolved anti-Stokes Raman signal for natural Ge (dotted line) and ^{70}Ge (solid line) at 80 K.

decays toward times prior to the arrival of the pump pulse, within the experimental uncertainty there is no difference in the in the phonon-population decay time between the natural Ge and ^{70}Ge samples. This time for both is $\tau=8\pm1$ ps. We have also measured a sample of natural Ge with a (100) surface. For this orientation only LO phonons are observed and the scattered light is orthogonally polarized with respect to the incident light. Consequently, polarization selection of the scattered light was used to discriminate against the Raman signal from the pump pulse. The corresponding time-resolved signal is shown in Fig. 5. The peak signal amplitude was 45 counts/s above the background signal. The time-dependent hot-luminescence signal was $\sim10\%$ of the peak signal. The data clearly show an asymmetry with the slower decay toward times following the pump pulse. It can also be seen that the signal does not decay to zero, but a constant signal remains. This constant signal was about 10% of the peak signal and experimentally reproducible. The decay toward longer times has a time constant $\tau\simeq8$ ps, in agreement with the two previously discussed samples.

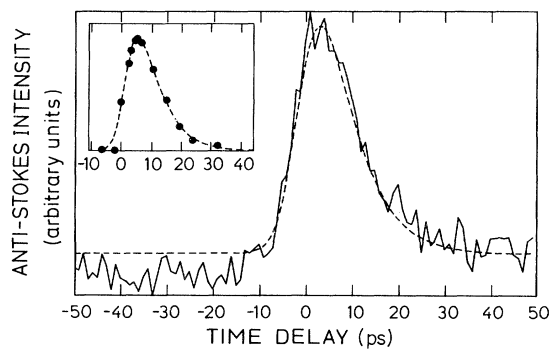

FIG. 5. Transient Raman signal for the (100) surface of natural Ge at 80 K. The dashed line is a modeled curve, details of which are described in the text. The inset shows data from Ref. 14 and a modeled curve (dashed line).

IV. DISCUSSION

A. Asymmetry of the optical Raman lines

The natural Ge as well as the isotopically enriched samples (95.9% ^{70}Ge, 86.0% ^{76}Ge) show an asymmetric first-order Raman line shape (see Fig. 3). Disorder-induced asymmetric optical-phonon lines in semiconductors have in the past only been observed in alloys, where the asymmetry has been attributed to disorder-induced phonons with a nonvanishing wave vector.[20,24]

The high accuracy of the measurements in this present work allowed an analysis of the asymmetry as a function of the isotopic composition of the different Ge samples. Figure 3 shows clearly that even the lines of the high-purity isotopically enriched samples were asymmetric. We propose two processes as being responsible for this asymmetry.

(i) Isotopic disorder: Because of contributions of the frequency-dependent self-energy in isotopically disordered systems, the line shape of first-order Raman scattering is asymmetric [see Sec. II, Eq. (4)].

(ii) Absorption of the incident laser light in the material: As discussed in Sec. II, the spatial confinement of the incident laser light results in a spread of the phonon wave vector, leading to an asymmetry of the Raman line [see Sec. II, Eq. (8)].

To combine both effects, the isotopic disorder and absorption, we used the model of Sec. II B in the analysis of the experimental data, with the modification that the half-width of the wave-vector spread, ξ, was considered to be the sum of a contribution from the absorption, α, and a contribution from the isotopic disorder, β:

$$\xi=\alpha+\beta\ . \tag{9}$$

The results of the wave-vector spread ξ, as obtained from fitting the experimental data to Eq. (8) (see Table II), were therefore interpreted as being the sum of the isotopic disorder and absorption contributions.

From ellipsometric measurements, the absorption coefficient in Ge at 100 K and a laser energy of 2.41 eV was determined to be $\alpha=590.4\times10^3$ cm^{-1}.[25] Subtracting this α from the fitted value of ξ yielded β, where β is the isotopic-disorder contribution to the asymmetry of the Raman line [Eq. (9)]. The isotopic-mass fluctuations are usually expressed by the g_2 factor, which is calculated in terms of the atomic masses m_i of the constituent isotopes (with concentrations x_i):

$$g_2=\sum_i x_i\left[1-\frac{m_i}{\bar{m}}\right]^2\ . \tag{10}$$

In Table III the isotopic asymmetry parameter β of the three samples is compared to g_2. For ^{70}Ge the asymmetry of the Raman line arises mainly from the finite penetration depth of the laser light in the material, for which the isotopic-disorder contribution is only about 3%. In the ^{76}Ge sample, the isotopic disorder contributed 19% to the asymmetry and 39% in natural Ge.

Comparing the ^{70}Ge sample with natural Ge, the isotopic contribution to the asymmetry of the Raman line β is

TABLE III. Comparison between the isotopic-mass disorder g_2 [see Eq. (10)] and the isotopic asymmetry parameter β [see Eq. (9)].

	g_2 (10^{-5})	$\frac{g_2}{g_2(\text{natural Ge})}$	β (10^3 cm^{-1})	$\frac{\beta}{\beta(\text{natural Ge})}$
^{76}Ge	8.797	0.150	135(±40)	0.36(±0.2)
Natural Ge	58.745	1.0	380(±50)	1.0
^{70}Ge	2.976	0.050 66	19(±30)	0.05(±0.1)

proportional to the isotopic-mass disorder g_2, whereas in the ^{76}Ge sample the isotopic disorder seems to contribute more to the asymmetry than expected from the isotopic-mass distribution. In all three samples, however, the predominant cause for the asymmetry of the first-order Raman line was the opacity of the material.

The theoretical curve (Fig. 1), calculated within the CPA using Eq. (4) and the phonon self-energies of Ref. 12, only takes into account asymmetry contributions due to isotopic disorder. Fitting the calculated line shape with the same procedure as the experimental results, the asymmetry parameter ξ was 1.33×10^6 cm^{-1}. This calculated asymmetry was larger than the experimental results by a factor of about 2, showing that the CPA somewhat overestimates the asymmetry due to isotopic disorder.

B. Anharmonic decay time and isotopic scattering time

The broadening of Raman lines is determined by the lifetime of the phonons. There are two processes which induce lifetime broadening of optical phonons: (i) spontaneous anharmonic decay into lower-energy phonons and (ii) elastic scattering due to isotopic disorder, defects, and impurities. We assume scattering due to defects and impurities to be negligible in our samples.

To distinguish the two contributions, we made use of the fact that the disorder scattering time τ_{isotope} is independent of the average isotopic mass of the material, but does depend on the isotonic composition (expressed in terms of the mass-fluctuation parameter g_2). The anharmonic decay time τ_{decay}, on the other hand, is proportional to the average mass, but is independent of the isotopic composition.[15]

We therefore write the FWHM of the modes Δ_{mode} obtained from the fits of Eq. (8) to the experimental data (see Table II) as

$$\Delta_{\text{mode}}=2\gamma=\frac{A}{\bar{m}}+g_2C=\frac{1}{2\pi c}\left[\frac{1}{\tau_{\text{decay}}}+\frac{1}{\tau_{\text{isotope}}}\right]. \quad (11)$$

The total linewidth of the modes was composed of the contribution $A/\bar{m}$ arising from the anharmonic decay and g_2C arising from isotopic disorder, where A and C were fitting parameters, g_2 is the mass-fluctuation parameter [see Eq. (10)], and c is the speed of light.

This is illustrated in Fig. 6, where the experimental Δ_{mode} were plotted as a function of the average atomic mass of the materials. Even though the differences between the FWHM's of the samples were small, the high accuracy of the measurements (0.02 cm^{-1}) allowed us to determine the decreasing linewidth with increasing atomic mass. The dashed line indicates the mass-dependent part of the phonon linewidth (due to anharmonic decay), $A/\bar{m}$, as obtained from fitting Eq. (11) to the experimental linewidths. The difference between this and the experimental data points arises from the isotopic-disorder scattering, which is mass independent, but depends on the isotopic-mass distribution [described by g_2; see Table III and Eq. (10)] and was therefore largest for natural Ge and smallest for the ^{70}Ge sample.

The FWHM broadening due to isotopic scattering of first-order Raman lines in natural Ge has been calculated by the self-consistent Born approximation to be 0.017 cm^{-1}.[12] This calculated result is in excellent agreement with the experimental value for the isotopic-disorder contribution to the Δ_{mode} in natural Ge of 0.024±0.02 cm^{-1} (see Fig. 6).

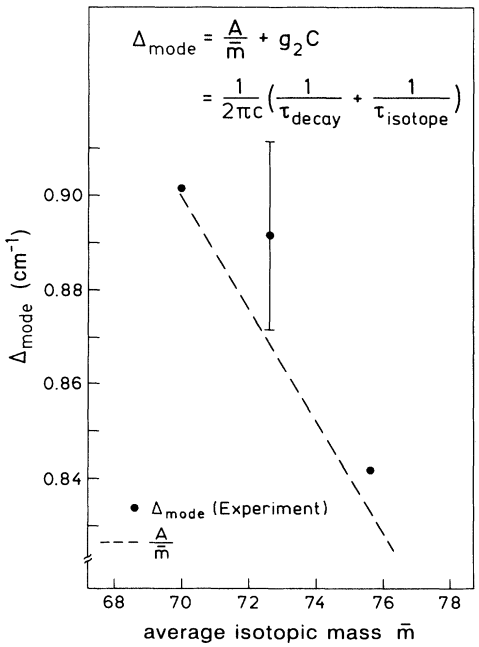

FIG. 6. Experimental, deconvoluted full widths at half maximum, $\Delta_{\text{mode}}=2\gamma$ [see Eq. (5)], of the modes for the isotopically enriched ^{76}Ge, ^{70}Ge, and natural Ge at 80 K with an excitation energy of $E_L=2.41$ eV (see Fig. 3). The points are experimental, one of them including the error bar. The dashed line indicates the mass-dependent part of the Δ_{mode} due to the anharmonic decay, whereas the difference between this line and the experimental data points is the isotopic-disorder scattering contribution (g_2C).

Converting the linewidths to the corresponding times, according to Eq. (11), we found the scattering time due to isotopic disorder as well as the anharmonic decay time for optical phonons in the Ge crystals of the different isotopic compositions. The results are listed in Table IV. The decay times of optical phonons were two orders of magnitude *smaller* than the average scattering time due to isotopic disorder. The lifetime (and hence the linewidth of the Raman lines) of optical phonons is therefore mainly determined by their decay time into lower-energy phonons. This result is in contrast with the calculated behavior of high-energy acoustic phonons in Ge whose decay time into lower-energy phonons is about 20 to 40 times *longer* than the isotopic scattering time.[1,2,6]

The time-resolved picosecond measurements of Fig. 4 show that, within the uncertainty of the experiment, the same phonon-population decay time of 8 ± 1 ps at 80 K was obtained for the natural as well as the isotopically enriched ^{70}Ge. The obtained decay time is in good agreement with previous time-resolved measurements.[10,11] Since the phonon lifetime is predominantly determined by the anharmonic decay, it is expected that *phonon-population* decay times measured in the time domain should agree with the *phonon* decay times determined from Raman linewidths. However, this is not the case (see Table IV). The difference between the decay times determined from time-resolved measurements and inverse linewidths of Raman spectra was previously attributed to isotopic-disorder scattering of optical phonons.[10] However, a comparison of Raman spectra from Ge crystals of different isotopic composition showed that this difference cannot be attributed to isotopic scattering (dephasing) of the phonons.[12] Because in this work the same samples were used for both experiments, the difference of the resulting decay times cannot be intrinsic to the sample, but must be due to the different experimental methods. We note that time-resolved spectra have previously been measured to be independent of the carrier density, up to 10^{20} cm^{-3}.[10] In the following section we consider the generation process of phonons in the picosecond experiment to explain the discrepancy between decay times measured in the frequency domain (anharmonic decay of phonons) and time domain (decay of nonequilibrium phonon population).

The experimentally determined phonon decay times agree well with previous calculations.[7,8] Cowley calculated the anharmonic decay time of optical phonons in Ge to be 12.5 ps at 10 K, 8.3 ps at 100 K, and 4 ps at 300 K,[26] taking into account all possible decay channels.[7] He used a shell model for the phonon density of states and axially symmetric forces between nearest neighbors to describe the anharmonic interaction.[7] Even though the shell-model description of the phonon dispersion is not very accurate,[15] the results compare well with the decay times found in this work. The calculations of Klemens[8] only take into account the decay of optical phonons into two acoustic phonons with opposite **q** vector which belong to the same branch. Using the same approximations that have been used for Si,[8] the calculations yield a decay time of optical phonons in Ge of 4.6 ps.[8] Considering the rough approximations in these calculations, it is not surprising that the decay times of Klemens are somewhat shorter than the experimentally observed ones.

TABLE IV. Anharmonic decay time and isotopic scattering time of optical phonons in the three Ge samples, determined from the experimental linewidths of the Raman spectra [see Eq. (11)].

	τ_{decay} (ps)	τ_{isotope} (ps)
^{76}Ge	6.4($\pm$0.1)	650($\pm$400)
Natural Ge	6.1($\pm$0.1)	220($\pm$200)
^{70}Ge	5.9($\pm$0.1)	3800($\pm$600)

As opposed to the time-resolved measurements, the frequency-domain spectra are sensitive to any process leading to inhomogeneous line broadening in addition to isotopic scattering and the finite penetration depth of light, such as inhomogeneous isotopic composition, impurities, or stress in the crystal. If errors in the results due to such processes are neglected, the method used in this work, namely, extracting the mass-dependent part from the FWHM of Raman spectra taken from Ge samples of various isotonic compositions under identical conditions, has an accuracy (about 3%) which is even better than that of typical time-dependent Raman measurements (10–20 %).

C. Carrier cooling and phonon generation in picosecond Raman experiments.

Carrier cooling in Ge at moderate carrier densities ($\sim10^{17}$ cm^{-3}) has been studied by photoinduced transmission experiments in which direct transitions in the Γ valley are bleached by the cooling hole plasma.[27] For a phonon energy $E_L=1.0$ eV, good agreement was found between experiment and a model invoking carrier cooling via deformation potential optical-phonon scattering. At a lattice temperature $T=120$ K, carrier cooling is completed in approximately 5 ps. Unfortunately, the model cannot account for transient transmission curves using larger photon energies ($E_L=2.1$ eV in this work), presumably because of the complexity of the band structure away from the Γ-valley minimum. In our time-resolved phonon measurements, the rate at which carriers cool and the concomittant generation of phonons may play an important role in explaining the discrepancy between the decay of the time-resolved signal and frequency linewidth. Recently, Othonos *et al.* modeled the temporal evolution of nonequilibrium phonon populations in Ge with a Boltzmann transport description, including a detailed account of the coupled carrier and phonon dynamics which give rise to the generation of Raman-detectable phonons.[14] However, they assumed the experimentally determined decay time of 8 ps for phonon relaxation. We consider that the generation and decay times for phonons in Ge are too similar to allow separable modeling. In the following analysis we focus on the asymmetric data shown in Fig. 5.

As a first approximation, we assume the following phonon-population rate equation:

$$\frac{\partial n}{\partial t} = \left[\frac{\partial n}{\partial t}\right]_{\text{gen}} - \left[\frac{\partial n}{\partial t}\right]_{\text{dec}} . \tag{12}$$

Without an independent measurement of carrier cooling after 2 eV photon excitation and detailed knowledge of which carrier cooling events produce Raman-detectable phonons, it is difficult to postulate a form for the generation term in Eq. (12); detailed modeling of the phonon generation was considered in Ref. 14. For simplicity, we have chosen an exponential generation rate

$$\left[\frac{\partial n}{\partial t}\right]_{\text{gen}} = \int_{-\infty}^{t} A I_p(t_1) \frac{e^{-(t-t_1)/\tau_g}}{\tau_g} dt_1 , \tag{13}$$

where $I_p(t_1)$ is the pump pulse intensity at time t_1, τ_g is the generation time constant, and A is the unknown efficiency factor for the generation of a Raman-detectable phonon per electron-hole pair. The decay rate is

$$\left[\frac{\partial n}{\partial t}\right]_{\text{dec}} = \int_{-\infty}^{t}\int_{-\infty}^{t_2} A I_p(t_1) \frac{e^{-(t_2-t_1)/\tau_g}}{\tau_g} \times \frac{e^{-(t-t_2)/\tau_d}}{\tau_d} dt_1 dt_2 , \tag{14}$$

where τ_d is the decay time. Finally, the total response must be convoluted with the temporal profile of the probe pulse.

Equation (12) has been solved numerically, and the result is displayed in Fig. 5 normalized to the data and with an offset to account for the constant long-time signal. The parameter values are $\tau_g = 3.5$ ps, $\tau_d = 6$ ps, and a laser pulse width of 5 ps. In addition, the curve has been shifted by 3 ps toward negative times due to experimental uncertainty in the determination of zero time delay. Shown in the inset of Fig. 5 are data taken from Ref. 14 and a normalized curve using the same generation and decay times, but with a pulse width of 4 ps (as reported for the measurement).

The good agreement between the simple model and the data brings to light an important consideration regarding the discrepancy between phonon decay times as measured in the frequency domain and the nonequilibrium phonon-population decay times as determined in the time domain. If a phonon decay time of 6 ps is assumed (as measured from the linewidths), then a reasonable account of the phonon-population decay data can be made with a phonon-generation time constant of 3.5 ps (see Fig. 5). We note that in GaAs the Fröhlich interaction enhances carrier cooling such that the relaxation is completed in approximately 2 ps;[9,28] consequently, the effect of prolonged phonon generation is not observed.

The long-time constant signal observed in Fig. 5 is further evidence that phonon-generation dynamics influence the time-resolved Raman signal. Pump-excited carriers which have cooled, but have neither recombined nor diffused out of the probed region, will undergo reheating via carrier-carrier scattering with the hot, probe-excited carriers. Subsequent cooling will generate new phonons which will be detected by the trailing edge of the probe pulse giving rise to a time-dependent signal. This signal will be sensitive to the diffusion of carriers out of the probed region of the specimen. Othonos *et al.*[14] have calculated that for an initial excitation density of 10^{18} cm^{-3} less than half of the carriers have diffused away from the surface after 20 ps. Incorporation of probe-induced reheating of carriers and the subsequent generation of observed phonons into our model requires detailed consideration of the time-dependent carrier plasma temperature and the phonon-generation process, both of which are beyond the scope of this first analysis. We note that in the previous time-resolved Raman measurements on GaAs by von der Linde, Kuhl, and Klingenberg[9] a similar effect was not observed since, at their carrier density (10^{17} cm^{-3}), carrier relaxation is dominated by carrier-phonon scattering rather than carrier-carrier scattering.[29]

The simple model we have used to describe the dynamics of the phonon population in Ge illustrates the need to consider phonon generation and decay simultaneously. In principle, the use of excitation photons with smaller energies will reduce the carrier cooling time, while a reduction in the probe pulse width will reduce the observed effect due to reheating of cool carriers from the pump pulse. Experiments in this direction are currently underway.

D. Phonon self-energy contributions due to isotopic disorder

The effect of isotopic disorder on the phonon energies can be described by the coherent-potential approximation, which, near Γ, gives results rather similar to those of the self-consistent Born approximation. The upward shift of the phonon energy in Ge of natural isotopic composition compared to the virtual crystal (perfect diamond-structure crystal with each site being occupied by a Ge atom of average atomic mass) has been calculated to be 1.5 cm^{-1} with the CPA (Ref. 12) and is 0.98 cm^{-1} with the SCBA, as shown in Sec. II A.

The difference of the observed phonon energies, as listed in Table II, include both the shift arising from the different average atomic masses in the samples and the self-energy contributions. Subtracting the simple mass dependence from the observed shifts, we obtained the self-energy contributions. Isotopic disorder also shifts the phonon energies in the isotopically enriched samples, even though this effect is small. Taking into account the isotopic disorder of the ^{76}Ge and ^{70}Ge samples, the results for the self-energy shifts of the optical zone-center phonons in natural Ge were 1.06 ± 0.04 cm^{-1} (with respect to ^{76}Ge) and 0.78 ± 0.04 cm^{-1} (with respect to ^{70}Ge). This is somewhat lower than the value of 1.5 cm^{-1} calculated with the CPA,[12] but agrees well with the 0.98 cm^{-1} calculated with the SCBA (Sec. II A). The different results obtained for this real self-energy by comparing natural Ge with ^{70}Ge and ^{76}Ge, respectively, may be the result of small temperature variations of the samples (the nitrogen cryostat allowed temperature variations of about 10 K, and so the difference of 0.16 cm^{-1} is well within the experimental uncertainty).

V. CONCLUSION

We have presented high-accuracy first-order Raman spectra taken from two different isotopically enriched Ge crystals (95.9% ^{70}Ge and 86.0% ^{76}Ge) and a Ge crystal of natural isotopic composition as well as time-resolved picosecond Raman spectra of the isotopically enriched ^{70}Ge and natural Ge sample. The line broadening, asymmetry, and energy of the Raman lines were investigated. The linewidth was found to be predominantly caused by the anharmonic decay of the optical phonons into lower-energy phonons, leading to a FWHM inversely proportional to the average atomic mass. From the linewidth of the Raman line, the anharmonic decay time was determined with high precision to be $\bar{m}(8.4\pm0.1)\times10^{-2}$ ps, where $\bar{m}$ is the average isotopic mass in atomic-mass units. The (elastic) isotope-disorder scattering time of the phonons is dependent on the mass fluctuation of the material and was found to be two orders of magnitude larger than the anharmonic decay time in all samples. The accuracy of the time-resolved picosecond spectra precluded the resolution of mass effects in the decay time. Consideration of the phonon-generation process was used to explain the discrepancy between the *phonon* decay time (as determined from the frequency-domain measurements) and the *phonon-population* decay time (as determined from the time-domain measurements). The asymmetric line shape of the Raman lines, also dependent on the isotopic composition, was explained with the opacity of the materials and with isotopic disorder. The broadening and shape as well as the phonon self-energy due to isotopic disorder were in agreement with calculations using the coherent-potential approximation and self-consistent Born approximation.

ACKNOWLEDGMENTS

We are thankful to V. Ozhogin for supplying the raw ^{70}Ge and to W. L. Hansen, E. E. Haller, and K. Itoh for growing the single crystal. Thanks are also due to H. V. Klapdor-Kleingrothaus, S. T. Belyaev, and V. Lebedev for the ^{76}Ge single crystal. We are also thankful to M. Siemers, P. Wurster, and H. Hirt for technical assistance. C.H.G. acknowledges partial support of the Natural Sciences and Engineering Research Council of Canada.

[1]S. Tamura, Phys. Rev. B **27**, 858 (1983).
[2]S. Tamura, Phys. Rev. B **31**, 2574 (1985).
[3]D. V. Kazakovtsek and Y. B. Levinson, Pis'ma, Zh. Eksp. Teor. Fiz. **27**, 194 (1978) [JETP Lett. **27**, 181 (1978)]; Phys. Status Solidi B **96**, 117 (1979).
[4]Y. B. Levinson, in *Nonequilibrium Phonons in Nonmetallic Crystals,* edited by W. Eisenmenger and A. A. Kaplyanski (North-Holland, Amsterdam, 1986).
[5]T. E. Wilson, F. M. Lurie, and W. E. Born, Phys. Rev. B **30**, 6103 (1984).
[6]H. J. Maris, Phys. Rev. B **41**, 9736 (1990).
[7]R. A. Cowley, J. Phys. (Paris) **26**, 659 (1965).
[8]P. G. Klemens, Phys. Rev. **148**, 845 (1966).
[9]D. von der Linde, J. Kuhl, and H. Klingenberg, Phys. Rev. Lett. **44**, 1505 (1980).
[10]L. Ye, C. B. Roxlo, and A. Z. Genack, Bull. Am. Phys. Soc. **32**, 934 (1987); A. Z. Genack, L. Ye, and C. B. Roxlo, Proc. Soc. Photo-Opt. Instrum. Eng. **942**, 130 (1988).
[11]J. F. Young, K. Wan, and H. M. van Driel, Solid-State Electron. **31**, 455 (1988).
[12]H. D. Fuchs, C. H. Grein, C. Thomsen, M. Cardona, W. L. Hansen, E. E. Haller, and K. Itoh, Phys. Rev. B **43**, 4835 (1991).
[13]V. F. Agekyan, V. M. Asnin, A. M. Kryukov, I. I. Markov, N. A. Rud', V. I. Stepanov, and A. B. Churilov, Fiz. Tverd. Tela (Leningrad) **31**, 101 (1989) [Sov. Phys. Solid State **31**, 2082 (1989)].
[14]A. Othonos, H. M. van Driel, J. F. Young, and P. Kelly, Phys. Rev. B **43**, 6682 (1991).
[15]J. Menéndez and M. Cardona, Phys. Rev. B **29**, 2051 (1984).
[16]J. R. Sandercock, Phys. Rev. Lett. **28**, 237 (1972).
[17]G. Dresselhaus and A. S. Pine, Solid State Commun. **16**, 1001 (1975).
[18]J. R. Sandercock, in *Light Scattering in Solids,* edited by M. Cardona and G. Güntherodt (Springer-Verlag, Berlin, 1982), Vol. 3.
[19]A. Dervish and R. Loudon, J. Phys. C **9**, L669 (1976).
[20]B. Jusserand and Jacques Sapriel, Phys. Rev. B **24**, 7194 (1981).
[21]G. Nilsson and G. Nelin, Phys. Rev. B **3**, 364 (1971).
[22]G. Abstreiter, M. Cardona, and A. Pinczuk, in *Light Scattering in Solids* (Ref. 18), Vol. 4.
[23]D. von der Linde, J. Kuhl, and E. Rosengart, J. Lumin. **24/25**, 675 (1981).
[24]P. Parayanthal and F. Pollak, Phys. Rev. Lett. **52**, 1822 (1984).
[25]L. Viña, S. Logothetidis, and M. Cardona, Phys. Rev. B **30**, 1979 (1984).
[26]The results of Ref. 7 as quoted in Ref. 15 are off by a factor of 2π because of a confusion of the different definitions of Γ. Cowley actually calculated the inverse lifetime $1/\tau$, and not the $\Delta_{\text{mode}}=2\Gamma$ of the spectra which would be $1/2\pi c\tau$.
[27]H. Roskos, B. Rieck, A. Seilmeier, and W. Kaiser, Appl. Phys. Lett. **53**, 2406 (1988); H. Roskos, B. Rieck, A. Seilmeier, and W. Kaiser, Solid-State Electron. **32**, 1437 (1989).
[28]J. A. Kash, J. C. Tsang, and J. M. Hvam, Phys. Rev. Lett. **54**, 2151 (1985).
[29]J. Shah, Solid-State Electron. **21**, 43 (1978).
[30]*CRC Handbook of Chemistry and Physics,* 57th ed., edited by R. C. Weast (CRC, Cleveland, 1976).